

Cite this: DOI: 10.1039/
d0md00034e

A₃- and A₂B-nitrocorroles: synthesis and antiviral activity evaluation against human cytomegalovirus infection†

Léo Bucher,^{‡a} Sandrine Kappler-Gratias,^{‡b} Nicolas Desbois,^{id a}
Kerstin Bystricky,^{id cd} Franck Gallardo^{*b} and Claude P. Gros^{id *a}

Human cytomegalovirus (hCMV) is responsible for several pathologies impacting immunocompromised patients and can trigger life-threatening infection. Several antivirals are available and are used in the clinic, but hCMV resistant strains have appeared and patients have encountered therapeutic failure. Hence, there is a constant need for new best in class or first in class antiviral molecules. We have previously shown that nitrocorroles could be used as a potent anti-hCMV agent without acute toxicity in mice. They therefore represent an excellent platform to perform structure–activity relationship (SAR) studies and to increase efficiency or reduce toxicity. We have generated original A₂B- and A₃-substituted nitrocorroles and have discovered optimized compounds with selectivity indices above 200. These compounds are easily synthesized in only one to two-step reactions; they are up-scalable and cost efficient. They are therefore excellent candidates for hCMV therapies and they pave the way for a new generation of molecules.

Received 29th January 2020,
Accepted 16th April 2020

DOI: 10.1039/d0md00034e

rsc.li/medchem

Introduction

The human cytomegalovirus (hCMV) is a DNA virus of the *Herpesviridae* family which currently infects nearly 80% of the world's population.^{1–8} Although infection is generally asymptomatic in immunocompetent persons, hCMV remains a major opportunistic pathogen in immunocompromised individuals. This is mainly the case of transplanted individuals in whom the infection can be life-threatening.⁹ In HIV infected patients, hCMV retinitis is the leading cause of blindness and the use of highly active antiretroviral therapy has strongly decreased hCMV associated complications. As for all herpes viruses, after primary infection, the virus persists in a lifelong latent state. The hCMV reservoir is known to be present in monocytes and CD34⁺ progenitors. Latent infection

reactivates in outbreaks that depend on environmental factors *e.g.* immune state and stress level. hCMV is a common virus that infects people of all ages and usually spreads from person to person through body fluids, such as blood, saliva, urine, semen, and breast milk. Most hCMV infections are usually silent, which means that the majority of people who are infected with hCMV have no signs or symptoms. However, pregnant women who are infected during the first quarter of pregnancy can transmit hCMV to their foetus, sometimes causing congenital hCMV infection.¹⁰ Congenital hCMV infection can cause problems from hearing loss to severe developmental and neuronal disabilities (resulting in some cases in foetal and neonatal death or in the development of serious clinical sequelae).¹⁰ In the US, hCMV infection is the first cause of congenital malformation and human cytomegalovirus today is still the leading non-genetic cause of congenital malformation in developed countries.

A current treatment of hCMV infection is based on a limited number of molecules that are mainly nucleotide or nucleoside analogues inhibiting viral DNA polymerase,¹¹ albeit new antiviral compounds with different mechanisms of action, such as letermovir, have been developed.³ Some of these compounds can have serious side effects, making them unsuited for widespread and repeated treatments. Resistant hCMV strains have also emerged, leading to therapeutic failure in some patients. The National Cytomegalovirus Research Center has estimated that 15% of patients either are non-responders to the proposed antiviral therapy or have to stop because of severe hematologic or renal toxicity.¹² It has been estimated that

^a Institut de Chimie Moléculaire de l'Université de Bourgogne (ICMUB), UMR CNRS 6302, Université Bourgogne Franche-Comté, 9 avenue Alain Savary, BP 47870, 21078 Dijon Cedex, France. E-mail: Claude.Gros@u-bourgogne.fr

^b NeoVirTech, SAS, 1 place Pierre Potier, Oncopole, 31106 Toulouse, France. E-mail: fgallardo@neovirtech.com

^c Centre de Biologie Intégrative (CBI), Laboratoire de Biologie Moléculaire Eucaryote (LBME), University of Toulouse, UPS, CNRS, Route de Narbonne, F-31062 Toulouse, France

^d Institut Universitaire de France (IUF), France

† Electronic supplementary information (ESI) available: ¹H and ¹⁹F NMR spectra, MALDI/TOF LRMS and ESI HR-MS spectra, and HPLC chromatograms of the reported corroles 1–17. Example of the algorithm used to detect and measure infection parameters. Miscellaneous precursor syntheses. See DOI: 10.1039/d0md00034e

‡ These are co-first authors.

Research Article

virological resistance represents 50% of the etiologies of non-response to treatment and concerns up to 7% of organ recipients treated in France and 3% of hematopoietic stem cell recipients.¹³ As a result, the development of new hCMV inhibitors, used in first line or in combination with pre-existing treatments, is a major public health issue.

Being interested in evaluating different corrole/porphyrin derivatives as potential inhibitors of the human cytomegalovirus (hCMV), we have previously screened over 200 porphyrinoid derivatives (*e.g.* porphyrin and corrole derivatives) against hCMV.¹⁴ Interestingly, strong antiviral and antiproliferative activities were detected for two hits: two nitro-corroles (isomers of the same corrole macrocycle) without acute *in vivo* toxicity.¹⁴ Indeed, daily injection in mice did not induce weight loss or any behaviour modifications. Although selectivity indices were not very high from these first-generation compounds, the nitro-corrole core is an interesting platform on which to perform structure–activity relationship studies in the aim of optimizing activity or decreasing toxicity.

We have focused our work on the synthesis and antiviral activity evaluation of a new generation of A₃- and A₂B-nitrocorroles, substituted by one or several additional halogen atoms at the *meso*-phenyl position of the corrole macrocycle. The relative ease of synthesis of free-base corrole macrocycles (from one-pot synthesis to only 2 steps) makes them ideal candidates for further antiviral studies.

Seventeen corroles were thus synthesized and tested for antiviral activity. A new series of A₃-corroles bearing a nitro EWG group either at the *ortho*-, *meta*- or *para*-positions was first prepared and fully characterized (Chart 1).

The later compounds differ by the position of one additional halogen atom (*e.g.* a fluorine atom in most cases but also a chlorine atom for one analog) or one additional electron-donating group (EDG: *e.g.* dimethylamine) or electron-withdrawing group (EWG: *e.g.* nitro, trifluoromethyl) substituents. Thanks to its peculiar properties,^{15–20} fluorine has been extensively studied and used in drug design and development. In medicinal chemistry, the nitro group is considered to be a unique and versatile functional group thanks to its strong electron attracting ability that creates localized electron deficient sites within molecules.²¹ The nitro group can also interact with different biological nucleophiles present in living systems, such as amino acids, nucleic acids, proteins and enzymes.²¹ A SAR study was carried out. As mentioned above, we have previously observed a *meso*-ring SAR for analogs of the tris-*para*-nitrophenyl corrole free base (previous hit); only analogs bearing at least one nitro, electron-withdrawing substituent, were potent (Scheme 1).

With the objective of interrogating the relevance of the A₃-substitution of the corrole scaffold, some A₂B-corroles were also synthesized wherein the aromatic group at the 10-*meso* position was replaced by a different phenyl-substituted ring, bearing in all cases a fluorine atom and a nitro group (Chart 1).

Overall, 11 compounds produced detectable antiviral activity against hCMV at a micromolar concentration (Tables 1 and 2).

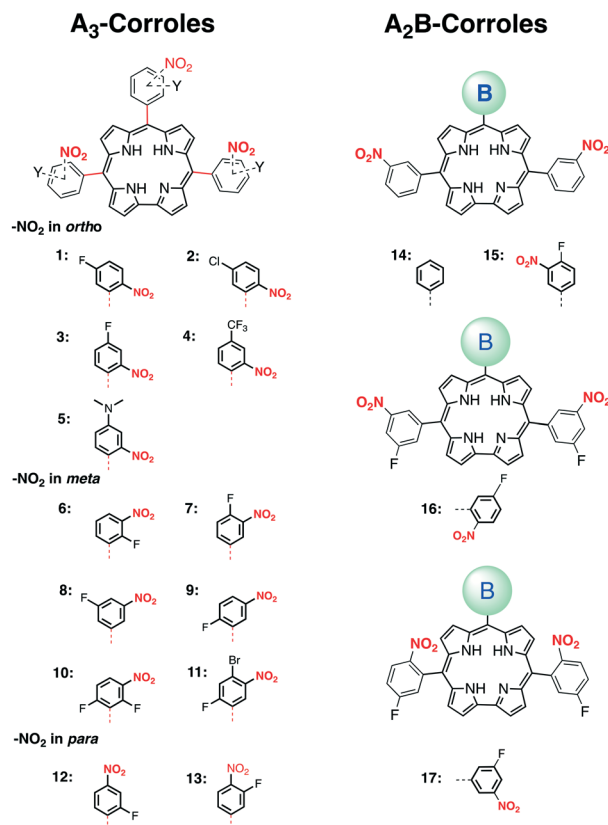
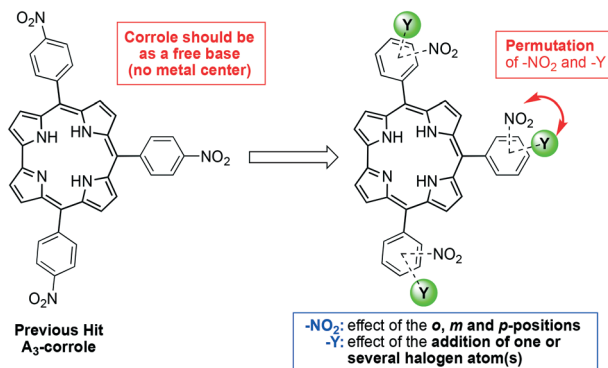


Chart 1 Structures of the A₃- and A₂B-fluoronitrocorroles.

Results and discussion

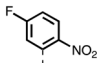
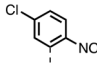
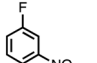
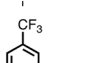
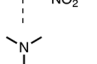
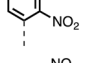
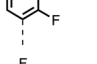
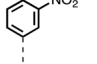
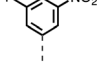
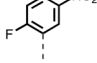
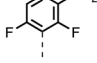
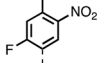
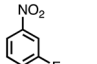
Chemistry

Two different procedures were used for the synthesis of the A₃-nitrocorroles^{22–24} and a third one for the synthesis of the A₂B-nitrocorroles (see Experimental section).²⁴ Indeed, the synthesis of the A₂B-corroles necessitates one additional step compared to that of the A₃-corroles and usually requires the synthesis of a dipyrromethane precursor.^{25–30} This latter can be synthesized by two main pathways. The first one consists in the use of a large excess of pyrrole (25 to 100 equivalents) and an acid catalyst.^{26,31} The second pathway allows the



Scheme 1 *meso*-Ring SAR for analogs of our previous hit.

Table 1 *In vitro* activity of A₃-corroles

A ₃ -Corroles					
Compound identity	A	Cell type	CC ₅₀ (μM)	IC ₅₀ (μM)	SI
1		MRC-5	>50	7.1 i	>7
		ARPE-19	>50	5.2 i	>10
2		MRC-5	>50	NE	—
		ARPE-19	>50	NE	—
3		MRC-5	>50	3 i	>16
		ARPE-19	>50	4.3 i	>11
4		MRC-5	>50	2.8 i	>17
		ARPE-19	>50	5 i	>10
5		MRC-5	>50	NE	—
		ARPE-19	>50	NE	—
6		MRC-5	>50	1.8 i	>27
		ARPE-19	>50	0.6 i	>82
7		MRC-5	>50	NE	—
		ARPE-19	>50	NE	—
8		MRC-5	>50	NE	—
		ARPE-19	>50	1.9 i	>26
9		MRC-5	3.7	1.5 i	2.4
		ARPE-19	50	1.3 i	39
10		MRC-5	8.77	0.86 i	10.20
		ARPE-19	9.80	0.31 i	31.61
11		MRC-5	>50	NE	—
		ARPE-19	>50	NE	—
12		MRC-5	3.4	0.7 i	4.5
		ARPE-19	5.3	0.25 i	21.2
13		MRC-5	>50	NE	—
		ARPE-19	>50	NE	—

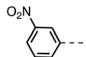
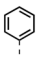
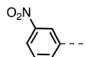
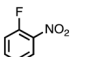
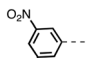
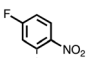
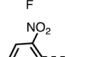
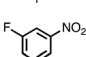
i = infection, NE = no effect. Value >50 means that CC₅₀ is above the maximum concentration tested.

synthesis of dipyrromethanes simply by mixing 1 equivalent of arylaldehyde with 2.5 equivalents of pyrrole in water in the presence of acid,^{29,32} leading (after reaction) to the precipitation of the dipyrromethane and easy filtration of the corrole precursor. The synthesis of A₂B-corroles consists in mixing one equivalent of arylaldehyde with two equivalents of dipyrromethane in a methanol/water mixture (which varies from 1:1 for dipyrromethanes to 2:1 for sterically hindered dipyrromethanes) with an excess of hydrochloric acid for one to two hours (the amount engaged being twice as large when a hindered dipyrromethane is used).²⁴ The bilane

precipitation is observed, which is further extracted with chloroform and oxidized with *p*-chloranil (or DDQ).²⁴ All A₃- and A₂B-corroles were fully characterized by ¹H NMR (as well as ¹⁹F NMR in some cases), low and high resolution (MALDI/TOF and ESI-MS, respectively), and by HPLC analysis to address the question of purity.

The SAR study that we first pursued resulted in A₃-corroles varying in the position and number of one lipophilic halogen group (*e.g.* -F, -Br or -Cl halogen atoms) and one nitro group on the *meso*-phenyl substituent, the corrole core being kept as a free-base as shown in Scheme 1

Table 2 *In vitro* activity of A₂B-corroles

A ₂ B-Corroles						
Compound identity	A	B	Cell type	CC ₅₀ (μM)	IC ₅₀ (μM)	SI
14			MRC-5	>50	NE	—
			ARPE-19	>50	NE	—
15			MRC-5	>50	NE	—
			ARPE-19	>50	5 i	>10
16			MRC-5	18	NE	—
			ARPE-19	16.5	0.32	51
17			MRC-5	>50	2 i	>25
			ARPE-19	>50	0.22 i	>227

i = infection, NE = no effect. Value >50 means that CC₅₀ is above the maximum concentration tested.

and Chart 1. As an example, corroles 7, 8 and 9 differ only in the position of the fluorine from the *para* to *meta* and then the *ortho*-position of the phenyl ring. Corrole 4 can be seen as a derivative of corrole 3 by increasing the electro-attractive (–I) inductive effect of the *para*-substituent. In corrole 5, the fluorine atom of 3 has been replaced by a dimethylamino EDG. Some A₂B-fluoronitro-corroles were also prepared in order to investigate any key effects of the substituents at the 10-*meso* position as well as any effects also of the symmetry of the corrole. Four A₂B-fluoronitrocorroles 14–17 were prepared by varying the nature of the aryl substituents at the 5,15-*meso* positions (Chart 1). As an example, corrole 16, an A₂B-corrole, can be considered as a hybrid between corrole 1 and corrole 8, shifting at the B *meso*-position one (and only one) nitro-group from the *meta* to the *ortho*-position.

In vitro activity

We have previously shown that mono-substituted nitrocorroles displayed antiviral activity against hCMV *in vitro*.¹⁴ This first-generation compound was used as a platform to synthesize several di- or tri-substituted nitrocorroles, either with A₃- or A₂B-geometry (symmetry). To further investigate the antiviral potency of the synthesized compounds, two cell lines that mimic hCMV infection were used: MRC-5 cells (primary human fibroblast) and ARPE-19 (retinal cell line). We first started by assessing the efficiency of a di-substituted fluoronitro-A₃-corrole derivative against hCMV infection in MRC-5. Cells were treated with increasing concentration of test compound 9 and immediately infected with ANCHOR hCMV at a multiplicity of infection MOI of 1. ANCHOR is a new DNA labeling technology^{33,34} which enables live cell visualization of the whole infection cycle, from infection to replication and propagation, of the fluorescently labeled virus.³⁵ Cells were cultured for 6 days following infection, then fixed and processed for high content imaging.

Fixation was required to stain nuclei and conserve plates until imaging. Infection rates and virus replication levels were scored by quantification of the ANCHOR hCMV fluorescence intensity using a compartmental analysis algorithm coupled with a spot detector. Imaging clearly display antiviral effects, with a global decrease in the infection rate and replication center intensity in cells treated with compound 9 compared to untreated cells (Fig. 1A, left).

High content quantification confirms that infection is reduced by 60% at the maximum concentration of compound 9 and that replication decreases up to 80% (Fig. 1B, middle). Treatment with compound 9 triggers a strong drop in cytopathic effect (data not shown), confirming that compound 9 display a true antiviral effect and does not interfere with the ANCHOR system. Toxicity assessment for the synthesized compounds indicates that this compound can be toxic at high concentration, with a cytotoxic concentration CC₅₀ at 3.69 μM (Fig. 1B, bottom) in MRC-5. However, compound 9 still displays potent antiviral activity at lower concentrations. In ARPE-19 cells, compound 9 displays very strong antiviral activity, triggering a 10-fold reduction of the infection rate and 5-fold reduction of the replication level (Fig. 1A right and C). The toxicity of the compound in the ARPE-19 cell line was clearly lower than that in MRC-5 with a CC₅₀ of 22.41 μM. Therefore, the selectivity index in ARPE-19 was higher, as high as 39 vs. 2.4 in MRC-5 cells. Several variants of compound 9 were then generated, mainly di- or tri-substituted A₃- or A₂B-nitrocorroles, most of them having at least one fluorine atom on a phenyl-substituent. This second generation of fluoronitrocorroles was then assessed for both toxicity and antiviral activity, as described for compound 9. Newly synthesized compounds with increased selectivity indices (either showing an increase in antiviral activity and/or a decrease of the toxicity) were expected.

To score toxicity, we plated MRC-5 and ARPE-19 cells and treated cells with increasing concentrations of test compounds 24 h post seeding. Cells were then fixed 6 days

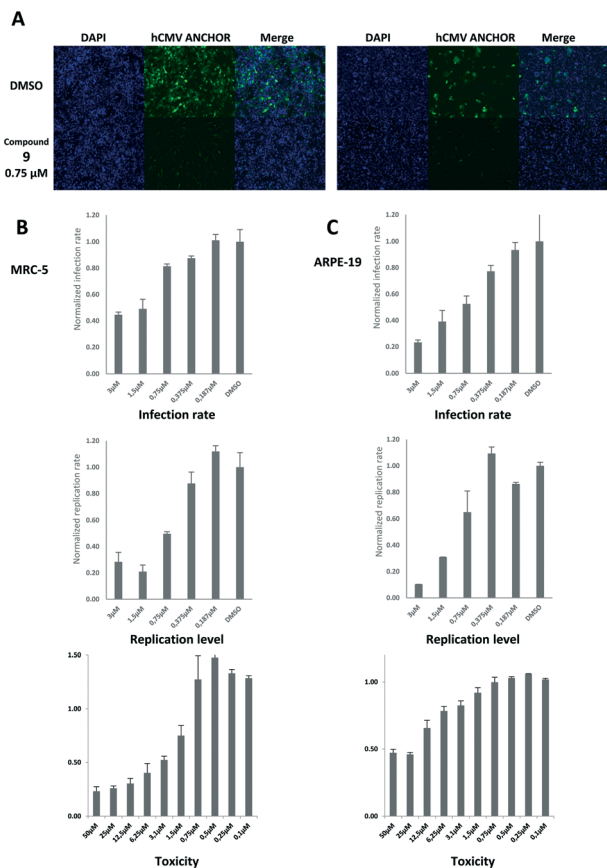


Fig. 1 Identification of fluoro-nitrocorroles as potent anti-hCMV inhibitors. A) MRC-5 cells (left) and ARPE-19 cells (right) infected with hCMV and treated with the vehicle alone (DMSO) or compound **9** at 0.75 μM . B) Quantification of the infection rate (top), hCMV replication level (middle) and compound toxicity (bottom) of MRC-5 cells treated with compound **9** at an increasing concentration normalized under DMSO treated conditions 6 days post infection/treatment. C) Same as B, but ARPE-19 cells are used. Results are the average of three independent wells + SD.

post-treatment for MRC-5 and 10 days for ARPE-19, and stained with Hoechst 33342. Toxicity scoring was performed using the same incubation time as for antiviral evaluation. Nuclei were counted and fluorescence intensity were scored using a cell cycle algorithm Thermo Cellinsight CX7 microscope. Toxicity, *i.e.* CC_{50} , is expressed as the concentration reducing the counted nuclei of 50% under treated *versus* untreated conditions. All synthesized variants were tested using the same pipeline and results are presented in Tables 1 and 2. An example of results obtained for compound **6** is shown in Fig. 2.

In Fig. 2A, ARPE-19 cells (top) treated with the vehicle alone (DMSO, left) or compound **6** at 50, 12.5 or 3.1 μM are imaged. No significant impact on the cell health can be imaged at 12.5 μM or below. Quantification of nuclei number in treated *vs.* untreated cells revealed that the CC_{50} in ARPE-19 was above the maximal concentration tested (50 μM) after 6 days of treatment. Similar experiments were performed in MRC-5 cells (A, bottom and B, right) to calculate a CC_{50} above

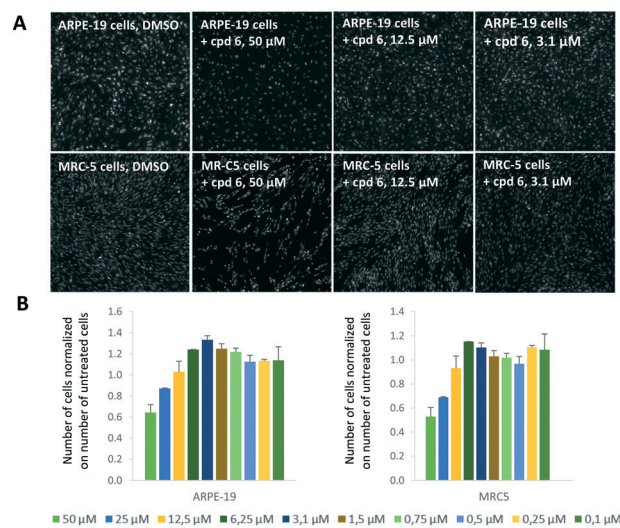


Fig. 2 Examples of toxicity testing of newly synthesized fluoro-nitrocorroles. A) ARPE-19 (top) and MRC-5 (bottom) treated with the vehicle alone (DMSO) or increasing concentration of compound **6**. Cells were fixed 6 days post-treatment and stained to visualize nuclei and typical images are shown. B) Calculation of the toxicity of compound **6** according to the number of nuclei count per well normalized under the vehicle treated conditions for ARPE-19 (left) and MRC-5 (right). Results are the average of two independent wells + SD.

50 μM 6 days post-treatment. The antiviral inhibition concentration IC_{50} of all variants was assessed as described for compound **9**.

Fig. 3 and 4 show examples of the antiviral effect of newly synthesized A_2B - and A_3 -fluorocorroles on hCMV infection in ARPE-19 and MRC-5 cells, respectively.

In Fig. 3, ARPE-19 cells treated with the vehicle alone display hCMV fluorescent plaques with very intense replication centers.

These plaques are completely abolished in the presence of compound **6** at 2.5 μM and are present but less intense at 1.25 μM . The presence of compound **17** at 1.25 μM prevents plaque propagation with few cells being infected. Compound **17** still displays a moderate effect at 0.3 μM . Compound **3** also displays a moderate effect but at higher concentration. The same trends can be observed in MRC-5 cells, as shown in Fig. 4. By using Thermo CellInsight compartmental analysis, coupled with a spot detector algorithm, we can determine the infection rate (the number of GFP positive cells over the total number of cells) and the viral DNA replication level (the integrated intensity of hCMV ANCHOR spots in the nucleus) of these compounds (Fig. 5). The infection rates in both MRC-5 and ARPE-19 cells decrease in a dose response manner for all compounds. While there is no impact on hCMV replication in MRC-5 cells, compounds also inhibit replication in ARPE-19 cells at high concentrations. This drop in replication may be linked to the increased incubation time for ARPE-19. As CC_{50} is above 50 μM for both cell lines with all three compounds, these compounds seem to be highly potent molecules to treat hCMV infection.

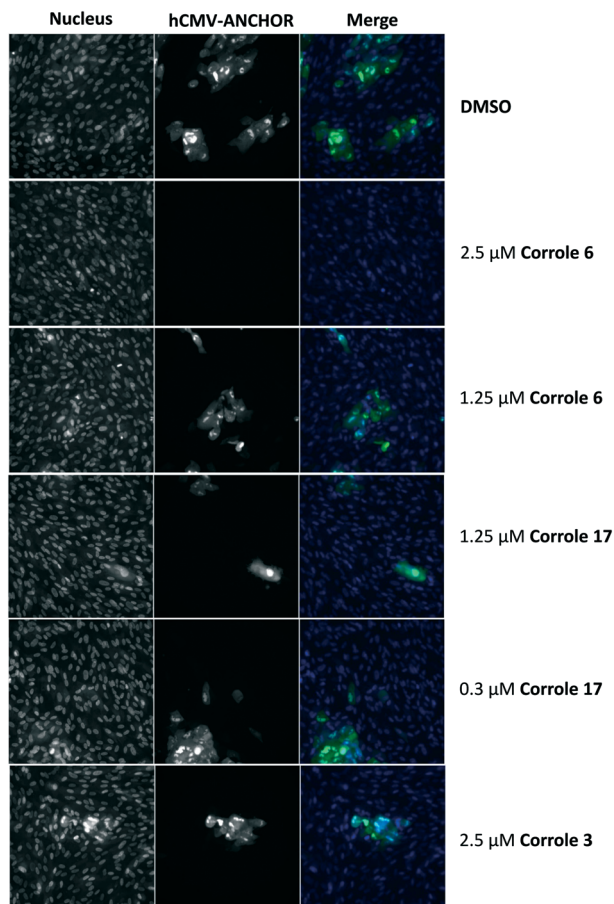


Fig. 3 Inhibitory effect of A_3 - and A_2B -corroles on hCMV infection in ARPE-19 cells. Cells were treated with different concentrations of indicated compounds and infected with hCMV ANCHOR for 10 days. Representative pictures are shown.

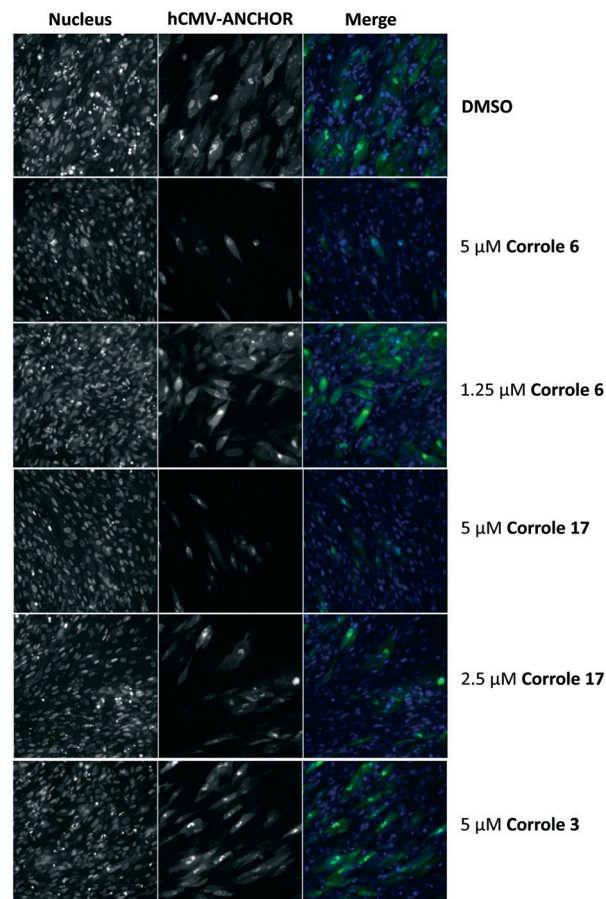


Fig. 4 Inhibitory effect of A_3 - and A_2B -corroles on hCMV infection in MRC-5 cells. Cells were treated with different concentrations of indicated compounds and infected with hCMV ANCHOR for 6 days. Representative pictures are shown.

Removing or replacing one fluorine atom completely abolishes the antiviral activity of the nitrocorroles (see compounds **14**, **5** and **2**). In addition, adding a bromine atom at the C4 *para*-phenyl position of compound **9** to create compound **11** abolishes the activity. Modifying the respective position of the fluorine and nitro groups in the A_3 - and A_2B -corroles can have a high impact. In general, the presence of a fluorine and a nitro group at the *ortho* position (relative to each other) correlates with a decrease in activity (compounds **7**, **13**, **15**), except for compound **6** which displays antiviral activity similar to compound **9** but reduced toxicity (in this latter corrole, the fluorine atom was shifted to the *ortho* position of the *meso*-phenyl ring). These results suggest that the relative positions of the $-NO_2$ and $-F$ groups are important in maintaining the activity. The best selectivity index (>227) is provided by compound **17**, an A_2B -nitrocorrole with $-F$ and $-NO_2$ in the *para* position (relative to each other) for A (phenyl ring) and in the *meta* position for B (phenyl ring, relative to each other). The difference in selectivity index between MRC-5 and ARPE-19 may reflect an increased sensitivity to the compound for MRC-5. The difference in activity may also be linked to a difference between the nature of the cell lines.

Indeed, ARPE-19 cells are epithelial whereas MRC-5 cells are fibroblasts; differences in the entry mechanism have been observed for hCMV between these two cell types.³⁶ Also, as the virus was produced in MRC-5 cells and is therefore adapted for fibroblasts, this may explain the high concentration needed to infect epithelial cells such as ARPE-19 and the propagation in the focal zone.³⁷ Adding an extra fluorine atom on compound **9** increases the antiviral effect in both cell lines, being almost two to four times stronger for compound **10** than for compound **9**. However, the CC_{50} of compound **10** also decreases and impacts the selectivity index. This finding therefore suggests that the presence of extra fluorine atoms on the *meso*-phenyl ring of the corrole macrocycle can greatly impact the antiviral activity.

Conclusions

In conclusion, starting from a nitro-corrole platform, we have synthesized and optimized variants displaying antiviral activity against hCMV with a SI of above 200. Out of these, 4 compounds achieved an IC_{50} at a nanomolar concentration (as low as 220 nM). The maximal activity is scored for ARPE-19 cell

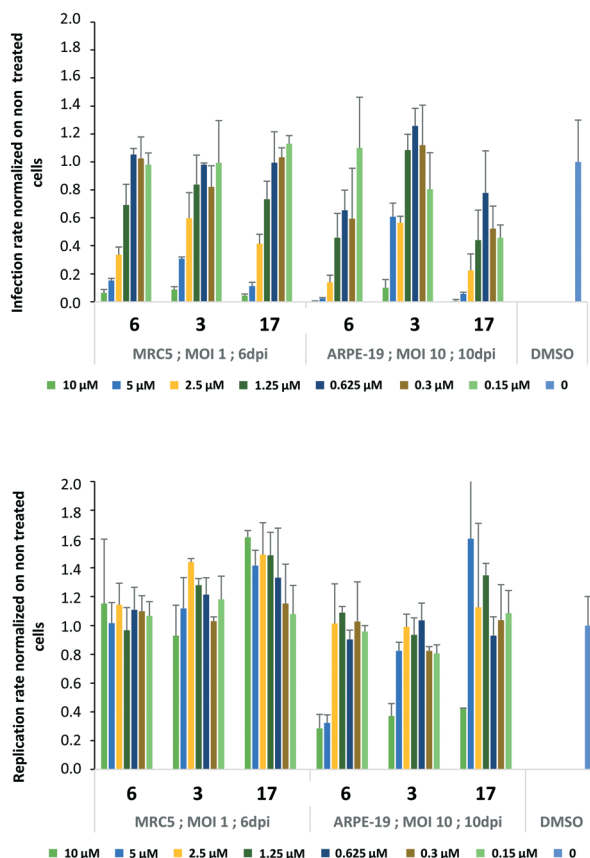


Fig. 5 A₃- and A₂B-corroles induce potent antiviral effects. Quantification of the infection rate (top) and hCMV replication levels of cells treated with the indicated dose of the compound normalized under DMSO treated conditions (either 6 dpi or 10 dpi, as indicated). Results are the average of two independent wells + SD.

lines, our model of hCMV retinitis, indicating that these compounds could be efficient in treating hCMV associated retinopathy where new treatment options are lacking. Related porphyrin analogs (*e.g.* verteporfin) are already used in combination with photodynamic therapy (PDT) for the treatment of wet age-related macular degeneration (AMD).^{38–41} Adding extra fluorine atoms on the corrole ring greatly increases the efficiency of the compound, indicating that the generated fluorinated variants may reach even greater antiviral potency and that their application should be further investigated.

Experimental

Cells, culture and media

MRC-5 human primary fibroblasts and ARPE-19 epithelial cells were purchased from ATCC (CCL171/CLR2302). Cells were grown in DMEM medium without phenol red (Sigma Aldrich), supplemented with 10% FBS, 1 mM sodium pyruvate, and 1× Glutamax (all from Gibco).

Toxicity assessment

Cells were plated at 8k per well in Corning Cellbind 96 well-plates in complete DMEM. 24 h post-seeding, cells were

treated with test compounds at the indicated concentration. Cells were then incubated at 37 °C and 5% CO₂ for 6 days. Following incubation, media were removed and cells are fixed with formalin (Sigma) for 10 min at RT. Cells were washed with PBS and incubated with PBS Hoechst 33342 (1 μg mL⁻¹). Cells were then imaged on a Thermo CellInsight CX7 HCS microscope using the cell cycle algorithm to count cell nuclei per condition. Results were extracted, normalized under the vehicle (DMSO) treated conditions and expressed as the average of two independent wells ± SD.

Screening of antiviral activities using high content imaging

The hCMV ANCHOR strain has been previously described.³⁵ ARPE-19 and MRC-5 cells were seeded at 8k cells per well in Corning Cell-bind glass bottom 96 well plates. 24 h post seeding cells were infected with 10 μL of hCMV ANCHOR dilution to reach a targeted multiplicity of infection MOI of 1 (MRC-5) or 10 (ARPE-19). 6 or 10 days post infection, cells were fixed as described in the toxicity section and imaged using a Thermo Scientific Cellinsight CX7 HCS microscope. A compartmental analysis coupled with a spot detector algorithm was used to detect and quantify the infection rate (number of fluorescent cells over total number of cells) and hCMV DNA replication level (integrated intensity of the hCMV ANCHOR spots). Results are displayed following automatic measurement of at least 1000 cells per well. Results are displayed as average of three independent wells ± SD.

Chemicals

2-Fluoro-4-nitrobenzaldehyde, 2,6-difluoro-3-nitrobenzaldehyde, 3-fluoro-5-nitrobenzaldehyde, 4-fluoro-2-nitrobenzaldehyde, 4-fluoro-2-nitrobenzaldehyde, 4-fluoro-3-nitrobenzaldehyde and 5-fluoro-2-nitrobenzaldehyde were purchased from Fluorochem. 5-Chloro-2-nitrobenzaldehyde, 2-nitro-4-(trifluoromethyl)benzaldehyde and 4-dimethylamine-2-nitrobenzaldehyde were purchased from Sigma-Aldrich. 2-Fluoro-5-nitrobenzaldehyde and 3-fluoro-4-nitrobenzaldehyde were purchased from Apollo Scientific. 4-Bromo-2-fluoro-5-nitrobenzaldehyde was purchased from Key Organics. 4-Nitrobenzaldehyde was purchased from Acros Organics. Benzaldehyde was purchased from Janssen Chimica.

Instrumentation

CDCl₃, THF-d₈, DMSO-d₆ and C₆D₆ were used as solvents for ¹H NMR spectra which were recorded on a Bruker AVANCE III spectrometer (500 MHz). The measurements were made at the PACSMUB-WPCM technological platform, which relies on the “*Institut de Chimie Moléculaire de l’Université de Bourgogne*” and Welience “TM”, a Burgundy University private subsidiary. Chemical shifts were expressed in ppm. Hydrazine hydrate was added to enhance the resolution of the spectra. Mass spectra were recorded on a Bruker Ultraflex Extreme MALDI Tandem TOF mass spectrometer using dithranol as the matrix or on a LTQ Orbitrap XL (Thermo) instrument in the ESI mode (for the HRMS spectra). HPLC

measurements were performed on a Dionex Ultimate 3000 system (Thermo Scientific). Condition #A: C18 Chromolith® SpeedROD column (Merck, 2 μm , 50–4.6 mm); 5 mL min^{-1} ; injected volume 2 μL ; wavelength detection: 400, 420, 440 nm or 465 nm; solvent A 0.1% TFA in H_2O ; solvent B acetonitrile. Conditions #B and #C: silica column (Syncronis, 3 μm , 150 \times 4.6 mm); flow rate 0.5 mL min^{-1} ; injected volume 2 μL ; wavelength detection: 420 nm, 465 nm; isocratic mode, solvent $\text{CHCl}_3/\text{MeOH}/\text{NET}_3$ (99.9/3/0.1) for condition #B and $\text{CHCl}_3/\text{MeOH}/\text{NET}_3$ (89.5/10/0.5) for condition #C.

General procedure A for the synthesis of A₃-corroles by Gryko's method²⁴

Aromatic aldehyde (1 equiv.) and freshly distilled pyrrole (2 equiv.) were added to MeOH (40 mL mmol^{-1} aldehyde) in an Erlenmeyer flask. An acidic mixture of H_2O (40 mL mmol^{-1} aldehyde) and HCl 37% (0.85 mL mmol^{-1} aldehyde) was introduced under vigorous agitation. The reaction mixture was allowed to stir in the dark at room temperature for 2 h, then extracted with CHCl_3 (3 \times 10 mL mmol^{-1} aldehyde), and washed with NaHCO_3 saturated aqueous solution (1 \times 20 mL mmol^{-1} aldehyde) and water (2 \times 15 mL mmol^{-1} aldehyde). The organic phase was further dried over MgSO_4 and the total volume of CHCl_3 was adjusted to 60 mL mmol^{-1} aldehyde. An oxidant was added to the solution in a round-bottom flask and left stirring overnight at room temperature. Hydrazine hydrate 64% (0.50 mL mmol^{-1} aldehyde) was added for 10 minutes before filtrating off insoluble materials over a Dicalite® plug. The solution was evaporated to dryness and the crude compound was then purified. The batch scale (amount of aldehyde), specific variations to the general procedure, and purification steps are detailed below for each compound.

General procedure B for the synthesis of A₃-corroles by Paolesse's method⁴²

Aromatic aldehyde (1 equiv.) and freshly distilled pyrrole (3 equiv.) were added to glacial acetic acid (12.5 mL mmol^{-1} aldehyde) in a round-bottom flask. The reaction mixture was refluxed in the dark for 3.5 h and the acetic acid was evaporated to dryness. The crude compound was directly purified afterwards. The batch scale (amount of aldehyde), specific variations to the general procedure, and purification steps are detailed below for each compound.

General procedure C for synthesis of A₂B-corroles by Gryko's method²⁴

Aromatic aldehyde (1 equiv.) and dipyromethane (2 equiv.) were dissolved in MeOH (100 mL mmol^{-1} aldehyde) in an Erlenmeyer flask. An acidic mixture of H_2O (100 mL mmol^{-1} aldehyde) and HCl 37% (5 mL mmol^{-1} aldehyde) was introduced under vigorous agitation. The reaction mixture was allowed to stir in the dark at room temperature for 1 h, then extracted with CHCl_3 (3 \times 50 mL mmol^{-1} aldehyde), and washed with NaHCO_3 saturated aqueous solution (1 \times 100

mL mmol^{-1} aldehyde) and water (2 \times 100 mL mmol^{-1} aldehyde). The organic phase was further dried over MgSO_4 and the total volume of CHCl_3 was adjusted to 500 mL mmol^{-1} aldehyde. An oxidant (3 equiv.) was added to the solution in a round-bottom flask and left stirring overnight at room temperature. Hydrazine hydrate 64% (1 mL mmol^{-1} aldehyde) was added for 10 minutes before filtrating off insoluble materials over a Dicalite® plug. The solution was evaporated to dryness and the crude compound was then purified. The batch scale (amount of aldehyde and dipyromethane), specific variations to the general procedure, and purification steps are detailed below for each compound.

5,10,15-Tris(5'-fluoro-2'-nitrophenyl)corrole 1. Corrole 1 was synthesized following general procedure A starting from 11.83 mmol (1 equiv., 2.00 g) of 5-fluoro-2-nitrobenzaldehyde. *p*-Chloranil (35.49 mmol, 3 equiv., 8.73 g) was chosen as the oxidant. The purification process used a SiO_2 plug (DCM) and a SiO_2 column (CHCl_3 /heptane 9:1) followed by recrystallization from heptane. Corrole 1 was isolated as a dark green solid with 1.0% yield (27 mg). UV/vis (CH_2Cl_2): λ_{max} (nm) ($\epsilon \times 10^{-3}$ L mol^{-1} cm^{-1}) = 412.9 (74.5), 574 (17.5), 611 (11.8), 647 (6.3). ^1H NMR (500 MHz, CDCl_3 + one drop of hydrazine hydrate 64%) δ (ppm): 8.97–8.90 (m, 2H), 8.62–8.34 (m, 9H), 8.08–7.95 (m, 3H), 7.54 (m, 3H). ^{19}F NMR (470 MHz, $\text{THF}-d_8$ + one drop of hydrazine hydrate 64%) δ (ppm): –108.09 to –109.86 (m, 3F). MS (MALDI-TOF, dithranol) m/z = 715.83 [$\text{M} + \text{H}$]⁺, 716.15 calcd for $\text{C}_{37}\text{H}_{21}\text{F}_3\text{N}_7\text{O}_6$. HR-MS (ESI) m/z = 716.1498 [$\text{M} + \text{H}$]⁺, 716.1500 calcd for $\text{C}_{37}\text{H}_{21}\text{F}_3\text{N}_7\text{O}_6$. HPLC (B): t_{R} = 3.3 min (purity 100% at 420 nm).

5,10,15-Tris(5'-chloro-2'-nitrophenyl)corrole 2. Corrole 2 was synthesized following general procedure B starting from 11.63 mmol (1 equiv., 2.16 g) of 5-chloro-2-nitrobenzaldehyde. The purification process used a SiO_2 plug (CHCl_3), a Bio-Beads® gel permeation chromatography column (SX-3, THF) and another SiO_2 column (CHCl_3 /heptane 7:3). Corrole 2 was isolated as a dark green solid with 0.7% yield (66 mg). UV/vis (CH_2Cl_2): λ_{max} (nm) ($\epsilon \times 10^{-3}$ L mol^{-1} cm^{-1}) = 414 (45.9), 578.1 (9.6), 610 (6.4), 643.7 (3). ^1H NMR (500 MHz, $\text{THF}-d_8$ + one drop of hydrazine hydrate 64%) δ (ppm): 8.94 (m, 2H), 8.57–8.23 (m, 12H), 7.91 (m, 3H). MS (MALDI-TOF, dithranol) m/z = 763.83 [$\text{M} + \text{H}$]⁺, 764.06 calcd for $\text{C}_{37}\text{H}_{21}\text{Cl}_3\text{N}_7\text{O}_6$. HR-MS (ESI) m/z = 764.0619 [$\text{M} + \text{H}$]⁺, 764.0613 calcd for $\text{C}_{37}\text{H}_{21}\text{Cl}_3\text{N}_7\text{O}_6$. HPLC (B): t_{R} = 3.8 min (purity 87% at 420 nm).

5,10,15-Tris(4'-fluoro-2'-nitrophenyl)corrole 3. Corrole 3 was synthesized following general procedure B starting from 14.78 mmol (1 equiv., 2.50 g) of 4-fluoro-2-nitrobenzaldehyde. The purification process used a SiO_2 plug (CHCl_3) and a Bio-Beads® gel permeation chromatography column (SX-3, THF) followed by recrystallization from a THF/heptane mixture. Corrole 3 was isolated as a dark green solid with 0.9% yield (30 mg). UV/vis (CH_2Cl_2): λ_{max} (nm) ($\epsilon \times 10^{-3}$ L mol^{-1} cm^{-1}) = 410 (73.7), 575.1 (13.9), 610 (9.1), 644.9 (4.1). ^1H NMR (500 MHz, $\text{THF}-d_8$ + one drop of hydrazine hydrate 64%) δ (ppm): 8.92 (m, 2H), 8.50–8.08 (m, 12H), 7.75 (m, 3H). ^{19}F NMR (470 MHz, $\text{THF}-d_8$ + one drop of hydrazine hydrate 64%) δ (ppm): –113.64 to –114.12 (m, 3F). MS (MALDI-TOF, dithranol) m/z =

716.14 [M + H]⁺, 716.15 calcd for C₃₇H₂₁F₃N₇O₆. HR-MS (ESI) *m/z* = 716.1514 [M + H]⁺, 716.1500 calcd for C₃₇H₂₀F₃N₇O₆. HPLC (B): *t_R* = 3.8 min (purity 97% at 420 nm).

5,10,15-Tris(2'-nitro-4'-trifluoromethyl)corrole 4. Corrole 4 was synthesized following general procedure B starting from 9.13 mmol (1 equiv., 2.00 g) of 2-nitro-4-(trifluoromethyl)-benzaldehyde. The purification process used a SiO₂ plug (CHCl₃) and a Bio-Beads® gel permeation chromatography column (SX-3, THF). Corrole 4 was isolated as a dark green solid with 1.0% yield (26 mg). UV/vis (CH₂Cl₂): λ_{max} (nm) (ε × 10⁻³ L mol⁻¹ cm⁻¹) = 414.9 (50.4), 576 (13.3), 611.7 (10), 655 (6.6), 742 (0.8). ¹H NMR (500 MHz, THF-*d*₈ + one drop of hydrazine hydrate 64%) δ (ppm): 8.93 (m, 2H), 8.67–8.39 (m, 10H), 8.26 (m, 5H). ¹⁹F NMR (470 MHz, THF-*d*₈ + one drop of hydrazine hydrate 64%) δ (ppm): -64.81 to -64.87 (m, 9F). MS (MALDI-TOF, dithranol) *m/z* = 866.40 [M + H]⁺, 866.14 calcd for C₄₀H₂₁F₉N₇O₆. HR-MS (ESI) *m/z* = 866.13923 [M + H]⁺, 866.14041 calcd for C₄₀H₂₁F₉N₇O₆. HPLC (B): *t_R* = 3.88 min (purity 91% at 420 nm).

5,10,15-Tris(4'-dimethylamino-2'-nitrophenyl)corrole 5. Corrole 5 was synthesized following general procedure A starting from 5.99 mmol (1 equiv., 1.16 g) of 4-dimethylamine-2-nitrobenzaldehyde. *p*-Chloranil (11.98 mmol, 2 equiv., 2.95 g) was chosen as the oxidant. The purification process used a SiO₂ column (CHCl₃) and Bio-Beads® gel permeation chromatography columns (SX-3, CHCl₃ then SX-1, CHCl₃) followed by recrystallization from an AcOEt/heptane mixture. Corrole 5 was isolated as a dark green solid with 2.2% yield (35 mg). UV/vis (CH₂Cl₂): λ_{max} (nm) (ε × 10⁻³ L mol⁻¹ cm⁻¹) = 407.1 (64.6), 630.1 (12.8). ¹H NMR (500 MHz, DMSO-*d*₆ + one drop of hydrazine hydrate 64%) δ (ppm): 8.78 (m, 2H), 8.34 (m, 2H), 8.22 (m, 2H), 8.10 (m, 3H), 7.95 (m, 2H), 7.48 (m, 3H), 7.31 (m, 3H), 3.21 (m, 18H). MS (MALDI-TOF, dithranol) *m/z* = 791.13 [M + H]⁺, 791.31 calcd for C₄₃H₃₉N₁₀O₆. HR-MS (ESI) *m/z* = 791.3050 [M + H]⁺, 791.3049 calcd for C₄₃H₃₉N₁₀O₆. HPLC (B): *t_R* = 3.8 min (purity 99.9% at 420 nm).

5,10,15-Tris(2'-fluoro-3'-nitrophenyl)corrole 6. Corrole 6 was synthesized following general procedure B starting from 8.87 mmol (1 equiv., 1.50 g) of 2-fluoro-3-nitrobenzaldehyde. The purification process used a SiO₂ plug (CHCl₃) and a Bio-Beads® gel permeation chromatography column (SX-3, THF) followed by recrystallization from a THF/heptane mixture. Corrole 6 was isolated as a dark green solid with 3.2% yield (67 mg). UV/vis (CH₂Cl₂): λ_{max} (nm) (ε × 10⁻³ L mol⁻¹ cm⁻¹) = 414 (11.2), 568.9 (19.1), 607.9 (9.6), 637.9 (4). ¹H NMR (500 MHz, THF-*d*₈ + one drop of hydrazine hydrate 64%) δ (ppm): 8.98 (m, 2H), 8.57–8.34 (m, 12H), 7.69 (m, 3H). ¹⁹F NMR (470 MHz, THF-*d*₈ + one drop of hydrazine hydrate 64%) δ (ppm): -120.22 to -121.91 (m, 3F). MS (MALDI-TOF, dithranol) *m/z* = 716.14 [M + H]⁺, 716.15 calcd for C₃₇H₂₁F₃N₇O₆. HR-MS (ESI) *m/z* = 716.1497 [M + H]⁺, 716.1500 calcd for C₃₇H₂₁F₃N₇O₆. HPLC (A): *t_R* = 6.2 min (purity 97% at 400 nm).

5,10,15-Tris(4'-fluoro-3'-nitrophenyl)corrole 7. Corrole 7 was synthesized following general procedure A starting from 13.38 mmol (1 equiv., 2.26 g) of 4-fluoro-3-nitrobenzaldehyde.

DDQ (13.38 mmol, 1 equiv., 3.04 g) was chosen as the oxidant. The purification process used a SiO₂ column (CHCl₃/heptane 9:1) and a Bio-Beads® gel permeation chromatography column (SX-3, THF) followed by recrystallization from a THF/heptane mixture. Corrole 7 was isolated as a dark green solid with 0.5% yield (15 mg). UV/vis (CH₂Cl₂): λ_{max} (nm) (ε × 10⁻³ L mol⁻¹ cm⁻¹) = 418.9 (84.9), 577 (13.4), 616.9 (8.4), 646.1 (5.7). ¹H NMR (500 MHz, THF-*d*₈ + one drop of hydrazine hydrate 64%) δ (ppm): 9.36 (m, 2H), 8.99–8.51 (m, 12H), 8.18 (m, 3H). ¹⁹F NMR (470 MHz, THF-*d*₈ + one drop of hydrazine hydrate 64%) δ (ppm): -116.49 (m, 2F), -124.87 (m, 1F). MS (MALDI-TOF, dithranol) *m/z* = 715.70 [M + H]⁺, 716.15 calcd for C₃₇H₂₁F₃N₇O₆. HR-MS (ESI) *m/z* = 716.1487 [M + H]⁺, 716.1500 calcd for C₃₇H₂₁F₃N₇O₆. HPLC (B): *t_R* = 3.8 min (purity 100% at 420 nm).

5,10,15-Tris(3'-fluoro-5'-nitrophenyl)corrole 8. Corrole 8 was synthesized following general procedure A starting from 5.91 mmol (1 equiv., 1.00 g) of 3-fluoro-5-nitrobenzaldehyde. *p*-Chloranil (11.83 mmol, 2 equiv., 2.91 g) was chosen as the oxidant. The purification process used a SiO₂ column (CHCl₃/petroleum ether 8:2) and a Bio-Beads® gel permeation chromatography column (SX-3, THF) followed by recrystallization from a DCM/heptane mixture. Corrole 8 was isolated as a dark green solid with 2.1% yield (30 mg). UV/vis (CH₂Cl₂): λ_{max} (nm) (ε × 10⁻³ L mol⁻¹ cm⁻¹) = 420.9 (76.2), 579 (15.1), 612.1 (8.9), 642 (5.6). ¹H NMR (500 MHz, THF-*d*₈ + one drop of hydrazine hydrate 64%) δ (ppm): 9.01 (m, 4H), 8.87 (m, 1H), 8.75 (d, *J* = 4.5 Hz, 2H), 8.62 (d, *J* = 4.0 Hz, 2H), 8.47 (m, 2H), 8.43 (d, *J* = 4.5 Hz, 2H), 8.33 (m, 2H), 8.24 (m, 2H). ¹⁹F NMR (470 MHz, THF-*d*₈ + one drop of hydrazine hydrate 64%) δ (ppm): -114.85 (t, *J* = 9.0 Hz, 2F), -116.05 (t, *J* = 9.0 Hz, 1F). MS (MALDI-TOF, dithranol) *m/z* = 715.86 [M + H]⁺, 716.15 calcd for C₃₇H₂₁F₃N₇O₆. HR-MS (ESI) *m/z* = 716.1501 [M + H]⁺, 716.1500 calcd for C₃₇H₂₁F₃N₇O₆. HPLC (B): *t_R* = 3.9 min (purity 100% at 420 nm).

5,10,15-Tris(2'-fluoro-5'-nitrophenyl)corrole 9. Corrole 9 was synthesized following general procedure B starting from 18.84 mmol (1 equiv., 3.18 g) of 2-fluoro-5-nitrobenzaldehyde. The purification process used a SiO₂ column (toluene/petroleum ether 9:1) and a Bio-Beads® gel permeation chromatography column (SX-3, THF) followed by recrystallization from a THF/ethanol mixture. Corrole 9 was isolated as a dark green solid with 3.7% yield (166 mg). UV/vis (CH₂Cl₂): λ_{max} (nm) (ε × 10⁻³ L mol⁻¹ cm⁻¹) = 416 (65.3), 570 (12.2), 609 (6.1), 638 (2.7). ¹H NMR (500 MHz, THF-*d*₈ + one drop of hydrazine hydrate 64%) δ (ppm): 9.03 (m, 5H), 8.59 (m, 5H), 8.50 (m, 2H), 8.34 (m, 2H), 7.72 (m, 3H). ¹⁹F NMR (470 MHz, THF-*d*₈ + one drop of hydrazine hydrate 64%) δ (ppm): -102.02 (m, 1F), -103.00 (m, 2F). MS (MALDI-TOF, dithranol) *m/z* = 714.82 [M]⁺, 715.14 calcd for C₃₇H₂₀F₃N₇O₆. HPLC (A): *t_R* = 6.4 min (purity 100% at 440 nm).

5,10,15-Tris(2',6'-difluoro-3'-nitrophenyl)corrole 10. Corrole 10 was synthesized following general procedure B starting from 6.80 mmol (1 equiv., 1.27 g) of 2,6-difluoro-3-nitrobenzaldehyde. The purification process used a SiO₂ plug (CHCl₃) and a Bio-Beads® gel permeation chromatography

column (SX-3, THF) followed by recrystallization from a THF/heptane mixture. Corrole **10** was isolated as a dark green solid with 4.0% yield (70 mg). UV/vis (CH₂Cl₂): λ_{\max} (nm) ($\epsilon \times 10^{-3} \text{ L mol}^{-1} \text{ cm}^{-1}$) = 410 (105.3), 563 (18.4), 605 (9.6), 655 (2.7). ¹H NMR (500 MHz, CDCl₃ + one drop of hydrazine hydrate 64%) δ (ppm): 9.07 (m, 2H), 8.71 (m, 2H), 8.58–8.53 (m, 7H), 7.52 (m, 3H). ¹⁹F NMR (470 MHz, CDCl₃ + one drop of hydrazine hydrate 64%) δ (ppm): –95.30 to –96.41 (m, 3F), –109.39 to –110.39 (m, 3F). MS (MALDI-TOF, dithranol) m/z = 769.95 [M + H]⁺, 770.12 calcd for C₃₇H₁₈F₆N₇O₆. HR-MS (ESI) m/z = 770.1213 [M + H]⁺, 770.1217 calcd for C₃₇H₁₈F₆N₇O₆. HPLC (A): t_{R} = 6.0 min (purity 100% at 440 nm).

5,10,15-Tris(4'-bromo-2'-fluoro-5'-nitrophenyl)corrole **11**.

Corrole **11** was synthesized following general procedure A starting from 4.05 mmol of 4-bromo-2-fluoro-5-nitrobenzaldehyde (1 equiv., 1.00 g). The purification process used a alumina plug (CHCl₃/heptane 8:2) and a Bio-Beads® gel permeation chromatography column (SX-3, THF) followed by recrystallization from an AcOEt/heptane mixture. Corrole **11** was isolated as a dark green solid with 0.9% yield (11 mg). UV/vis (CH₂Cl₂): λ_{\max} (nm) ($\epsilon \times 10^{-3} \text{ L mol}^{-1} \text{ cm}^{-1}$) = 420.9 (59.5), 571 (11.1), 609 (7.6), 645 (5). ¹H NMR (500 MHz, THF-*d*₈ + one drop of hydrazine hydrate 64%) δ (ppm): 8.95 (m, 2H), 8.80 (m, 3H), 8.59 (m, 2H), 8.51 (m, 2H), 8.36 (m, 2H), 8.06 (m, 3H). ¹⁹F NMR (470 MHz, THF-*d*₈ + one drop of hydrazine hydrate 64%) δ (ppm): –102.82 (m, 1F), –103.96 (m, 2F). MS (MALDI-TOF, dithranol) m/z = 949.61 [M + H]⁺, 949.88 calcd for C₃₇H₁₈BrF₃N₇O₆. HPLC (C): t_{R} = 3.6 min (purity 100% at 420 nm).

5,10,15-Tris(2'-fluoro-4'-nitrophenyl)corrole **12.** Corrole **12** was synthesized following general procedure B starting from 3.85 mmol (1 equiv., 650 mg) of 2-fluoro-4-nitrobenzaldehyde. The purification process used a SiO₂ plug (CHCl₃) and a Bio-Beads® gel permeation chromatography column (SX-3, THF) followed by recrystallization from a CHCl₃/heptane mixture. Corrole **12** was isolated as a dark green solid with 7.4% yield (68 mg). UV/vis (CH₂Cl₂): λ_{\max} (nm) ($\epsilon \times 10^{-3} \text{ L mol}^{-1} \text{ cm}^{-1}$) = 431 (65.5), 585.1 (23.3). ¹H NMR (500 MHz, THF-*d*₈ + one drop of hydrazine hydrate 64%) δ (ppm): 8.96 (m, 2H), 8.59 (m, 2H), 8.51 (m, 2H), 8.45–8.33 (m, 11H). ¹⁹F NMR (470 MHz, THF-*d*₈ + one drop of hydrazine hydrate 64%) δ (ppm): –110.16 to 110.52 (m, 1F), –111.14 to 111.75 (m, 2F). MS (MALDI-TOF, dithranol) m/z = 715.75 [M + H]⁺, 716.15 calcd for C₃₇H₂₁F₃N₇O₆. HR-MS (ESI) m/z = 716.1506 [M + H]⁺, 716.1500 calcd for C₃₇H₂₁F₃N₇O₆. HPLC (A): t_{R} = 6.5 min (purity 95% at 400 nm).

5,10,15-Tris(3'-fluoro-4'-nitrophenyl)corrole **13.** Corrole **13** was synthesized following general procedure B starting from 12.89 mmol (1 equiv., 2.18 g) of 3-fluoro-4-nitrobenzaldehyde. The purification process used a SiO₂ plug (CHCl₃/heptane 9:1) and a Bio-Beads® gel permeation chromatography column (SX-3, THF), followed by recrystallization from a CHCl₃/MeOH mixture with subsequent heptane washing. Corrole **13** was isolated as a dark green solid with 6.7% yield (205 mg). UV/vis (CH₂Cl₂): λ_{\max} (nm) ($\epsilon \times 10^{-3} \text{ L mol}^{-1} \text{ cm}^{-1}$) = 448 (74.3), 597 (23.5). ¹H NMR (500 MHz, CDCl₃) δ (ppm): 9.10 (m, 2H),

8.98 (m, 2H), 8.88 (s, 1H), 8.70 (m, 2H), 8.59–8.51 (m, 5H), 8.34 (m, 4H), 8.17 (m, 2H). ¹⁹F NMR (470 MHz, THF-*d*₈ + one drop of hydrazine hydrate 64%) δ (ppm): –120.39 (m, 2F), –121.81 (m, 1F). MS (MALDI-TOF, dithranol) m/z = 715.76 [M + H]⁺, 716.15 calcd for C₃₇H₂₁F₃N₇O₆. HR-MS (ESI) m/z = 716.1503 [M + H]⁺, 716.1500 calcd for C₃₇H₂₁F₃N₇O₆. HPLC (A): t_{R} = 6.5 min (purity 100% at 440 nm).

5,15-Bis(3'-nitrophenyl)-10-(phenyl)corrole **14.** Corrole **14** was synthesized following general procedure C starting from 3.74 mmol (1 equiv., 381.2 μ L) of benzaldehyde and 7.48 mmol (2 equiv., 2.00 g) of 5-(3'-nitrophenyl)-dipyrrromethane.²⁵ *p*-Chloranil (11.23 mmol, 3 equiv., 2.76 g) was chosen as the oxidant. The purification process used a SiO₂ plug (DCM) followed by recrystallization in a CHCl₃/EtOH mixture. Corrole **14** was isolated as a dark green solid with 49.5% yield (1.142 g). Corrole **14** was obtained according to a different protocol than the one previously reported in the literature.⁴³ ¹H NMR (500 MHz, THF-*d*₈ + one drop of hydrazine hydrate 64%) δ (ppm): 9.17 (m, 2H), 9.02 (m, 2H), 8.78 (m, 2H), 8.73 (m, 2H), 8.58 (m, 2H), 8.53 (m, 4H), 8.17 (m, 2H), 8.01 (m, 2H), 7.70 (m, 3H). MS (MALDI-TOF, dithranol) m/z = 616.83 [M + H]⁺, 617.20 calcd for C₃₇H₂₅N₆O₄. HR-MS (ESI) m/z = 617.1925 [M + H]⁺, 617.1932 calcd for C₃₇H₂₅N₆O₄. HPLC (B): t_{R} = 3.7 min (purity 84% at 420 nm).

5,15-Bis(3'-nitrophenyl)-10-(4'-fluoro-3'-nitrophenyl)corrole **15.** Corrole **15** was synthesized following general procedure C starting from 1.91 mmol (1 equiv., 323 mg) of 4-fluoro-3-nitrobenzaldehyde and 3.82 mmol (2 equiv., 1.03 g) of 5-(3'-nitrophenyl)-dipyrrromethane (3.82 mmol).²⁵ *p*-Chloranil (5.73 mmol, 3 equiv., 1.41 g) was chosen as the oxidant. The purification process used a SiO₂ plug (CHCl₃) followed by recrystallization in EtOH. Corrole **15** was isolated as a dark green solid with 28.0% yield (366 mg). UV/vis (CH₂Cl₂): λ_{\max} (nm) ($\epsilon \times 10^{-3} \text{ L mol}^{-1} \text{ cm}^{-1}$) = 418 (82.8), 578.1 (15.2), 616.9 (10.5), 646.9 (7.7). ¹H NMR (500 MHz, DMSO-*d*₆ + one drop of hydrazine hydrate 64%) δ (ppm): 9.03 (m, 4H), 8.70 (m, 4H), 8.63 (m, 1H), 8.57 (d, *J* = 4.0 Hz, 2H), 8.51 (d, *J* = 8.5 Hz, 2H), 8.46 (d, *J* = 4.0 Hz, 2H), 8.32 (d, *J* = 8.5 Hz, 1H), 8.09 (t, *J* = 7.5 Hz, 2H), 7.95 (d, *J* = 8.5 Hz, 1H). ¹⁹F NMR (470 MHz, THF-*d*₈ + one drop of hydrazine hydrate 64%) δ (ppm): –126.09 (s, 1F). MS (MALDI-TOF, dithranol) m/z = 679.78 [M + H]⁺, 680.17 calcd for C₃₇H₂₃FN₇O₆. HR-MS (ESI) m/z = 680.1686 [M + H]⁺, 680.1688 calcd for C₃₇H₂₃FN₇O₆. HPLC (B): t_{R} = 3.8 min (purity 100% at 420 nm).

5,15-Bis(3'-fluoro-5'-nitrophenyl)-10-(5'-fluoro-2'-nitrophenyl)corrole **16.** Corrole **16** was synthesized following general procedure C starting from 1.45 mmol (1 equiv., 245 mg) of 5-fluoro-2-nitrobenzaldehyde and 2.89 mmol (2 equiv., 825 mg) of 5-(3'-fluoro-5'-nitrophenyl)-dipyrrromethane. DDQ (4.35 mmol, 3 equiv., 987 mg) was chosen as the oxidant. The purification process used a SiO₂ plug (CHCl₃) followed by recrystallization in a CHCl₃/heptane mixture. Corrole **16** was isolated as a dark green solid with 32.8% yield (340 mg). UV/vis (CH₂Cl₂): λ_{\max} (nm) ($\epsilon \times 10^{-3} \text{ L mol}^{-1} \text{ cm}^{-1}$) = 420.9 (92), 580 (18.8), 618 (11), 650.7 (5.7). ¹H NMR (500 MHz, THF-*d*₈ + one drop of hydrazine hydrate 64%) δ (ppm): 9.04 (m, 4H),

8.76 (d, $J = 4.5$ Hz, 2H), 8.65 (d, $J = 4.0$ Hz, 2H), 8.49 (m, 2H), 8.38 (m, 3H), 8.29 (td, $J = 2.0$ Hz, $J = 9.0$ Hz, 2H), 8.04 (dd, $J = 3.0$ Hz, $J = 9.0$ Hz, 1H), 7.67 (m, 1H). ^{19}F NMR (470 MHz, THF- d_8 + one drop of hydrazine hydrate 64%) δ (ppm): -110.89 (s, 1F), -114.56 (s, 2F). MS (MALDI-TOF, dithranol) $m/z = 715.78$ $[\text{M} + \text{H}]^+$, 716.15 calcd for $\text{C}_{37}\text{H}_{21}\text{F}_3\text{N}_7\text{O}_6$. HR-MS (ESI) $m/z = 716.1500$ $[\text{M} + \text{H}]^+$, 716.1450 calcd for $\text{C}_{37}\text{H}_{21}\text{F}_3\text{N}_7\text{O}_6$. HPLC (B): $t_{\text{R}} = 3.9$ min (purity 96% at 420 nm).

5,15-Bis(5'-fluoro-2'-nitrophenyl)-10-(3'-fluoro-5'-nitrophenyl)corrole 17. Corrole 17 was synthesized following general procedure C starting from 2.66 mmol (1 equiv., 450 mg) of 3-fluoro-5-nitrobenzaldehyde (2.66 mmol) and 5.32 mmol (2 equiv., 1.52 g) of 5-(5'-fluoro-2'-nitrophenyl)-dipyrrromethane. DDQ (7.98 mmol, 3 equiv., 1.81 g) was chosen as the oxidant. The purification process used a SiO_2 plug ($\text{CHCl}_3/\text{cyclohexane}$ 8:2) and a Bio-Beads® gel permeation chromatography column (SX-3, THF) followed by recrystallization in a $\text{CHCl}_3/\text{heptane}$ mixture. Corrole 17 was isolated as a dark green solid with 48.3% yield (612 mg). Notably, the purified compound is composed of several atropisomers. It has to be noted that the atropisomers were not easily separable (we tried but were not successful) and the isolation of the atropisomers was not the purpose of this SAR study. UV/vis (CH_2Cl_2): λ_{max} (nm) ($\epsilon \times 10^{-3}$ L mol $^{-1}$ cm $^{-1}$) = 412.9 (44.2), 575.1 (9.3), 607.9 (5.9), 646.3 (2.7). ^1H NMR (500 MHz, THF- d_8 + one drop of hydrazine hydrate 64%) δ (ppm): 8.92 (m, 3H), 8.59 (m, 2H), 8.41 (m, 8H), 8.10 (m, 2H), 7.64 (m, 2H). ^{19}F NMR (470 MHz, THF- d_8 + one drop of hydrazine hydrate 64%) δ (ppm): -108.03 to -108.86 (m, 3F), -113.82 (m, 1F). MS (MALDI-TOF, dithranol) $m/z = 715.79$ $[\text{M} + \text{H}]^+$, 716.15 calcd for $\text{C}_{37}\text{H}_{21}\text{F}_3\text{N}_7\text{O}_6$. HR-MS (ESI) $m/z = 716.1506$ $[\text{M} + \text{H}]^+$, 716.1500 calcd for $\text{C}_{37}\text{H}_{21}\text{F}_3\text{N}_7\text{O}_6$. HPLC (B): $t_{\text{R}} = 3.9$ min (purity 95% at 420 nm).

Conflicts of interest

The authors declare no competing financial interest.

Acknowledgements

Support was provided by the CNRS (UMR 6302), the "Université Bourgogne Franche-Comté" and the "Conseil Régional de Bourgogne" through the PARI Project. French Technology Transfer Organization Sayens (SATT) and Mrs. Marie Petit are gratefully acknowledged through the VIRCO project. We are really thankful to Mrs. Claire Bernhard for valorization advices and to Mrs. Sandrine Pacquelet for technical assistance. The authors wish also to thank the "Plateforme d'Analyse Chimique et de Synthèse Moléculaire de l'Université de Bourgogne" (PACSMUB, <http://www.wpcm.fr>) for access to analytical instrumentation. We wish to express our gratitude to Dr. Quentin Bonnin and Mrs. Marie-José Penouilh for HR-MS measurements. We finally want to warmly thank Mrs. Mary Bouley for the final reading of the article (English correction).

Notes and references

- 1 E. De Clercq and L. Naesens, *J. Clin. Virol.*, 2006, **37**, S82–S86.
- 2 E. Denes and S. Ranger-Rogez, *Expert Rev. Anti-infect. Ther.*, 2005, **3**, 663–678.
- 3 T. Goldner, G. Hewlett, N. Ettischer, H. Ruebsamen-Schaeff, H. Zimmermann and P. Lischka, *J. Virol.*, 2011, **85**, 10884–10893.
- 4 D. P. Melendez and R. R. Razonable, *Infect. Drug Resist.*, 2015, **8**, 269–277.
- 5 L. Pilorge, S. Burrel, Z. Ait-Arkoub, H. Agut and D. Boutolleau, *Antiviral Res.*, 2014, **111**, 8–12.
- 6 H. Sabit, A. Dahan, J. Sun, C. J. Provoda, K. D. Lee, J. H. Hilfinger and G. L. Amidon, *Mol. Pharmaceutics*, 2013, **10**, 1417–1424.
- 7 M. R. Schleiss, D. I. Bernstein, M. A. McVoy, G. Stroup, F. Bravo, B. Creasy, A. McGregor, K. Henninger and S. Hallenberger, *Antiviral Res.*, 2005, **65**, 35–43.
- 8 K. Zarrouk, J. Piret and G. Boivin, *Virus Res.*, 2017, **234**, 177–192.
- 9 C. N. Kotton, D. Kumar, A. M. Caliendo, A. Asberg, S. Chou, L. Danziger-Isakov and A. Hum, *Transplantation*, 2013, **96**, 333–360.
- 10 S. T. Hamilton, W. van Zuylen, A. Shand, G. M. Scott, Z. Naing, B. Hall, M. E. Craig and W. D. Rawlinson, *Rev. Med. Virol.*, 2014, **24**, 420–433.
- 11 M. Boeckh, W. J. Murphy and K. S. Peggs, *Biol. Blood Marrow Transplant.*, 2015, **21**, S19–S24.
- 12 E. Shmueli, R. Or, M. Y. Shapira, I. B. Resnick, O. Caplan, T. Bdolah-Abram and D. G. Wolf, *J. Infect. Dis.*, 2014, **209**, 557–561.
- 13 B. A. Krishna, M. R. Wills and J. H. Sinclair, *Br. Med. Bull.*, 2019, **131**, 5–17.
- 14 C. P. Gros, N. Desbois, C. Michelin, E. Demilly, A. F. Tilkin-Mariame, B. Mariame and F. Gallardo, *ACS Infect. Dis.*, 2015, **1**, 350–356.
- 15 E. P. Gillis, K. J. Eastman, M. D. Hill, D. J. Donnelly and N. A. Meanwell, *J. Med. Chem.*, 2015, **58**, 8315–8359.
- 16 E. A. Ilardi, E. Vitaku and J. T. Njardarson, *J. Med. Chem.*, 2014, **57**, 2832–2842.
- 17 N. A. Meanwell, *J. Med. Chem.*, 2018, **61**, 5822–5880.
- 18 C. D. Murphy, *Appl. Microbiol. Biotechnol.*, 2016, **100**, 2617–2627.
- 19 J. Wang, M. Sanchez-Rosello, J. L. Acena, C. del Pozo, A. E. Sorochinsky, S. Fustero, V. A. Soloshonok and H. Liu, *Chem. Rev.*, 2014, **114**, 2432–2506.
- 20 Y. Zhou, J. Wang, Z. N. Gu, S. N. Wang, W. Zhu, J. L. Acena, V. A. Soloshonok, K. Izawa and H. Liu, *Chem. Rev.*, 2016, **116**, 422–518.
- 21 K. Nepali, H. Y. Lee and J. P. Liou, *J. Med. Chem.*, 2019, **62**, 2851–2893.
- 22 R. Paolesse, S. Nardis, F. Sagone and R. G. Khoury, *J. Org. Chem.*, 2001, **66**, 550–556.
- 23 R. Paolesse, A. Marini, S. Nardis, A. Froiio, F. Mandoj, D. J. Nurco, L. Prodi, M. Montalti and K. M. Smith, *J. Porphyrins Phthalocyanines*, 2003, **07**, 25–36.

- 24 B. Koszarna and D. T. Gryko, *J. Org. Chem.*, 2006, **71**, 3707–3717.
- 25 C. Drexler, M. W. Hosseini, A. De Cian and J. Fischer, *Tetrahedron Lett.*, 1997, **38**, 2993–2996.
- 26 J. K. Laha, S. Shanalekshmi, M. Taniguchi, A. Ambroise and J. S. Lindsey, *Org. Process Res. Dev.*, 2003, **7**, 799–812.
- 27 B. J. Littler, M. A. Miller, C.-H. Hung, D. F. O'Shea and J. S. Lindsey, *J. Org. Chem.*, 1999, **64**, 1391–1396.
- 28 Z. Liu, I. Schmidt, P. Thamyongkit, R. S. Loewe, D. Syomin, J. R. Diers, Q. Zhao, V. Misra, J. S. Lindsey and D. F. Bocian, *Chem. Mater.*, 2005, **17**, 3728–3742.
- 29 T. Rohand, E. Dolusic, T. H. Ngo, W. Maes and W. Dehaen, *ARKIVOC*, 2007, 307–324.
- 30 A. J. F. N. Sobral, N. G. C. L. Rebanda, M. da Silva, S. H. Lampreia, M. Ramos Silva, A. M. Beja, J. A. Paixão and A. M. D. A. Rocha Gonsalves, *Tetrahedron Lett.*, 2003, **44**, 3971–3973.
- 31 B. S. Lee and J. S. Lindsey, *Tetrahedron: Asymmetry*, 1994, **50**, 11427–11440.
- 32 V. Král, P. Vašek and B. Dolenský, *Collect. Czech. Chem. Commun.*, 2004, **69**, 1126–1136.
- 33 H. Saad, F. Gallardo, M. Dalvai, N. Tanguy-le-Gac, D. Lane and K. Bystricky, *PLoS Genet.*, 2014, **10**, e1004187.
- 34 T. Germier, S. Kocanova, N. Walther, A. Bancaud, H. A. Shaban, H. Sellou, A. Z. Politi, J. Ellenberg, F. Gallardo and K. Bystricky, *Biophys. J.*, 2017, **113**, 1383–1394.
- 35 B. Mariame, S. Kappler-Gratias, M. Kappler, S. Balor, F. Gallardo and K. Bystricky, *J. Virol.*, 2018, **92**, e00571-18.
- 36 B. J. Ryckman, M. C. Chase and D. C. Johnson, *Proc. Natl. Acad. Sci. U. S. A.*, 2008, **105**, 14118–14123.
- 37 L. Scrivano, C. Sinzger, H. Nitschko, U. H. Koszinowski and B. Adler, *PLoS Pathog.*, 2011, **7**, e1001256.
- 38 J. W. Miller, U. Schmidt-Erfurth, M. Sickenberg, C. J. Pournaras, H. Laqua, I. Barbazetto, L. Zografos, B. Piguët, G. Donati, A. M. Lane, R. Birngruber, H. van den Berg, A. Strong, U. Manjuri, T. Gray, M. Fsadni, N. M. Bressler and E. S. Gragoudas, *Arch. Ophthalmol.*, 1999, **117**, 1161–1173.
- 39 U. Schmidt-Erfurth and T. Hasan, *Surv. Ophthalmol.*, 2000, **45**, 195–214.
- 40 M. S. Dhalla, K. J. Blinder, G. K. Shah and J. Wickens, *US Sensory Disorders Rev.*, 2006, pp. 7–12.
- 41 R. Wormald, J. Evans, L. Smeeth and K. Henshaw, *Cochrane Database Syst. Rev.*, 2003, vol. 3, p. CD002030.
- 42 R. Paolesse, L. Jaquinod, D. J. Nurco, S. Mini, F. Sagone, T. Boschi and K. M. Smith, *Chem. Commun.*, 1999, 1307–1308.
- 43 D. T. Gryko, M. Tasior and B. Koszarna, *J. Porphyrins Phthalocyanines*, 2003, **7**, 239–248.